

# 3D EM MODELLING – APPLICATION OF THE LOCALIZED NON-LINEAR APPROXIMATOR TO NEAR SURFACE APPLICATIONS

*Ross Groom and Catalina Alvarez, PetRos EiKon Inc, Milton, ON*

## Abstract

The development of rapid  $O(N)$  numerical techniques, initiated by the pioneering of the Localized Non-Linear (LN) Approximator in 1993 (Habashy, Groom and Spies [1]), has offered many possibilities for the simulation of realistic electromagnetic situations for a wide range of applications. At the beginning, very rapid calculation times combined with minimal memory requirements offered the potential to simulate more complex and thus more geologically meaningful models. This continues today. However, new possibilities and capabilities continue to evolve. We have experimented with many developments in LN techniques (Murray et al [4]), including extensions to inductive modes, multi-body problems, time-varying and static magnetic effects and polyhedral primitives. Although the technique was initially developed for hydrocarbon reservoir characterization and later for mineral exploration, the techniques are proving useful for near-surface environmental and geotechnical applications.

Our general formulation provides extensions of the technique to simulation problems of specific interest for near-surface EM. In particular, induction effects due to contrasts solely in induced magnetization and the combined response due to contrasts in resistivity and magnetization. The use of our original techniques as well as research into new extensions as they pertain to near-surface applications will be discussed.

## Introduction

To simulate three-dimensional electromagnetic scattering in the earth, either differential or integral equation techniques are used. In terms of the large and often ill-conditioned matrices that must be generated and solved, the difficulties arising in standard approaches are well known. This was the impetus behind the initial development of the Localized Non-Linear (LN) Approximator (Habashy, Groom and Spies [1]).

While the early developments of the LN technique indicated the tremendous potential of the method, the original formulation provided only what is sometimes called the current channelling or galvanic response. By deriving the magnetic field from the internal electric currents, inductive responses were poorly estimated (Murray [2]). This limitation is, however, common to most electric field formulations.

The early LN technique provided excellent representations of full wave internal field scattering for secondary galvanic responses in the case of a single spherical scatterer. The algorithm was later extended to right rectangular prisms of arbitrary aspect ratio (Groom, Walker and Dyck [3]) thus providing the building blocks for more realistic and complex models. To fully implement the LN algorithm, techniques were required to handle multi-body interactions. Then, for a wider range of models to be tractable, a more amorphous type of scattering primitive was required (a non-convex polyhedron) and the inability of the technique to model inductive responses had to be addressed.

In many environmental applications of EM, conductivity is not always the only factor governing the response of anomalous bodies. Although, the original LN technique considered variations in conductivity and electrical permittivity, magnetic (susceptibility) variations can also play a role. Algorithms, which can tolerate simultaneous variations in all electrical properties, are extremely important for many geophysical applications of electromagnetics and extensions of the LN are possible for these problems.

# Electromagnetic Response Modes and Extensions of Non-Linear Approximator

## Extension to Stronger Inductive Modes

We first begin with the integral representation of the electric field both internal and external to the scatterer

$$E(r) = E_b(r) + \int dr' \overline{\overline{G}}(r, r') \bullet Q(r') E(r') \quad (1)$$

$$\nabla \times \nabla \times E_b - k_b^2 E_b = i\omega \mu_0 J_s + \nabla \times M_s \quad .$$

The LN Approximator estimates the internal field inside regions of anomalous conductivity by assuming that

$$E(r) \approx \nabla E_b(r) + \nabla \int dr' \overline{\overline{G}}(r, r') \bullet Q(r') E(r) \quad (2)$$

at a given observation point, only the local *value* of the field is important, and this value (which is unknown) is extrapolated across the target. Of course, the LN technique is accurate only when the local *gradients* (and higher order derivatives of the internal field) are truly insignificant. Certainly, for a strong inductive coupling of source and scatterer, the effects of the field gradients are of importance, and in such cases the LN approximation will be inadequate. That is, for any internal point,  $r$ ,

Where,  $Q$ , is the complex conductivity:

$$Q(r) = i\omega \mu_0 [ \sigma(r) - \sigma_b ] + \omega^2 \mu_0 [ \epsilon(r) - \epsilon_b ]$$

Thus allowing the representation of the internal field by an analytic scattering operator

$$E(r) = \overline{\overline{\Gamma}}(r) E_b(r) = \left[ \overline{\overline{I}} - \overline{\overline{QL}} \right]^{-1} E_b(r), \quad \overline{\overline{L}} = \int_{V(i)} dr' \overline{\overline{G}} \quad (2)$$

The scattering operator,  $\Gamma$ , is dependent on the geometry of the scatterer, the position of the internal point and the complex frequency. Thus, its derivation sometimes requires some mathematical effort but thereafter is computed relatively free and provides in some instances some considerable improvements in accuracy. It also allows for the calculation of the magnetic field directly by integrating over the appropriate Greens' tensor times the internal electric field determined by Eq. (2). In this section, we assume that the magnetic permeability  $\mu$  is constant throughout the medium and take the curl of Eq(2) and use Eq(1) to obtain

$$\nabla^* E(r) = \nabla E_b(r) + Q \nabla \int dr' \overline{\overline{G}} \bullet E(r') \quad (3)$$

When induction is significant, the gradients in the internal electric field cannot be neglected when performing the integral in Eq (1) to determine the internal electric field. To estimate the effect of the internal gradients, we proceed as follows. If the contrast  $Q(r)$  is uniform over the scatterer, then formally taking spatial derivatives of Eq(4) yields, in a shorthand notation

$$\nabla^* E = \nabla^* E_b + Q \nabla^* \int dr' \overline{\overline{G}} \bullet [E(r) + \nabla E(r) \bullet (r' - r)] \quad (4)$$

where the gradient operator  $\nabla^* = [1, \nabla] = [1, \partial/\partial x, \partial/\partial y, \partial/\partial z]$ . By Taylor expansion, Eq (4) can be written as a set of equations in the form

$$\sum_{j=i}^4 \overline{\overline{T}}_{ij} \bullet V_j = F_i, \quad i = 1, 2, 3, 4 \quad (5)$$

$V_i$  and  $F_i$  are three-space vectors and  $\overline{\overline{T}}_{ij}$  are 3x3 matrices. Hence, Eqs.(5) constitutes a 12x12 linear system in the unknowns  $v_i$ ,  $i = 1,2,3,4$ . The tensorial expressions  $\overline{\overline{T}}_{ij}$  are functions of the geometrical and electrical properties of the scatterer, and of  $r$  and  $\omega$ . They are semi-analytic in nature, expressible as a combination of analytical and numerical quadratures. This extension, we term the ILN approximation.

### Extension to Multiple Targets:

A single scatterer is often insufficient to represent realistic earth situations and in such cases, the superposition of responses is only valid for multiple targets which are sufficiently spatially separated. When utilizing multiple targets in conventional techniques, one can often observe that interactions between anomalies are non-physical.

For multiple targets (not in contact), the effect of interaction (to first order) can be calculated as follows. Consider a model of two structures in some proximity, and imagine a receiver at a location internal to the first anomaly. The receiver is energized with the host field (the field in the absence of both scatterers) plus a first order backscatter from the second structure and vice versa. This analysis is first-order; in reality the interaction series is infinite. However, evaluating more than the primary backscattering contribution is computationally expensive and often unnecessary. In particular, a converged series is necessary when the targets are in close proximity (and it is in this case where many numerical techniques often fail) but the LN algorithms already have a unique sense for this interaction: current is obliged by the technique to flow between the structures.

To put these concepts on a firmer foundation, consider calculating the scattered field for a collection of  $n$  conductivity anomalies and for the sake of argument, multiple LN prism scatterers each with uniform electrical properties. Treated separately, the LN approximation [1] says that the internal field inside prism  $i$  is

$$E^{(i)} = \overline{\overline{\Gamma}}^{(i)} E_b^{(i)} = \left[ \overline{\overline{I}} - Q^{(i)} \overline{\overline{L}}^{(i)} \right]^{-1} E_b^{(i)}, \quad \overline{\overline{L}}^{(i)} = \int_{V^{(i)}} dr' \overline{\overline{G}}, \quad i = 1, n$$

For the collection of prisms, it is consistent with the LN approximation that for a point inside the aggregate structure the internal field is given by

$$E = \left[ \overline{\overline{I}} - \sum_{j=1}^n \overline{\overline{L}}^{(j)} Q^{(j)} \right]^{-1} E_b$$

The scattered electric field is then represented as

$$E_s = \sum_{i=1}^n \int_{V^{(i)}} dr' \overline{\overline{G}} \cdot \left[ \overline{\overline{I}} - \sum_{j=1}^n Q^{(j)} \overline{\overline{L}}^{(j)} \right]^{-1} E_b^{(i)} \quad (6)$$

When targets are in close proximity, it is more persuasive physically to replace  $Q^{(i)}$  with  $Q^{(j)}$  inside the integral in Eq.(6). This would then give the secondary field as

$$E_{s,NF} = \sum_{i=1}^n \int_{V^{(i)}} dr' \overline{\overline{G}} \cdot \left[ \overline{\overline{I}} - Q^{(i)} \sum_{j=1}^n \overline{\overline{L}}^{(j)} \right]^{-1} E_b^{(i)} \quad (7)$$

This multiple scattering technique is termed *Near Field* interactions, and represents continuous current flow between scatterers. Although an approximation, it has proven effective in representing data in these situations.

There are other ways to incorporate multiple scattering. For instance, the field interior to the  $i^{th}$  object can be

approximated via

$$E^{(i)} [ \bar{I} - Q^{(i)} \bar{L}^{(i)} ] = E_b^{(i)} + \sum_{j \neq i}^n \int_{V^{(j)}} dr' \bar{G} \cdot E^{(j)}$$

(where the terms in the summation can be considered as secondary sources) or

$$E^{(i)} = \bar{\Gamma}^{(i)} [ E_b^{(i)} + \sum_{j \neq i}^n \int_{V^{(j)}} dr' \bar{G} \cdot E^{(j)} ]$$

giving the expression for the scattered field under single scattering, which we term *Far Field* interactions:

$$E_{s, FF} = \sum_{i=1}^n \int_{V^{(i)}} dr' \bar{G}(r, r') \cdot \bar{\Gamma}^{(i)} \cdot [ E_b^{(i)} + \sum_{j \neq i}^n \int_{V^{(j)}} dr' \bar{G}(r', r'') \cdot \bar{\Gamma}^{(j)} E_b^{(j)} ] \quad (8)$$

Note that without the internal summation in Eq.(8) the result is simply the superposed scattered field, that is to say

$$E_{s, SP} = \sum_{i=1}^n \int_{V^{(i)}} dr' \bar{G} \cdot \bar{\Gamma}^{(i)} E_b^{(i)} \quad (9)$$

is the response of the combined targets in *Superposition*.

### Extension to Magnetic Effects

In Maxwell's equations, when we allow a contrast in permeability, we cannot (profitably) take the curl of Ampere's Law as in the *Inductive Modes* section. If the scatterer is only magnetic or only permeability contrasts play a role, as in static (DC) magnetics, we can by analogy take the curl of Faraday's and Ampere's law in an equivalent procedure. For variations in conductivity, permittivity and permeability, we require a new approach, namely we write the basic equations as

$$\nabla \times H = \Delta \sigma^* E + \sigma_b^* E + J_s \quad (10)$$

$$\nabla \times E = \Delta \mu^* H + \mu_b^* H + M_s \quad (11)$$

where (for now) we assume the host medium has constant parameters  $\sigma_b$ ,  $\epsilon_b$ , and  $\mu_b$ , and define

$$\Delta \sigma^* = \sigma^* - \sigma_b^* = [\sigma - i\omega\epsilon] - [\sigma_b - i\omega\epsilon_b] = \Delta\sigma - i\omega\Delta\epsilon$$

$$\Delta \mu^* = \mu^* - \mu_b^* = [i\omega\mu] - [i\omega\mu_b] = i\omega\Delta\mu$$

$$Q^H = \sigma_b^* \Delta \mu^*$$

$$Q^E = \mu_b^* \Delta \sigma^*$$

We now decompose the fields as

$$H = H_0 + H_*, E = E_0 + E_*$$

where

$$\nabla \times H_0 = \sigma_b^* E_* + J_s \quad (12)$$

$$\nabla \times H_* = \Delta \sigma^* [E_0 + E_*] + \sigma_b^* E_0 \quad (13)$$

$$\nabla \times E_0 = \mu^* H_* + M_s \quad (14)$$

$$\nabla \times E_* = \Delta \mu^* [H_0 + H_*] + \mu_b^* H_0 \quad (15)$$

so that  $H_0$  and  $E_0$  have the familiar solutions

$$H_0 = H_0^b + \int dr' \overline{\overline{G}} \bullet Q^H H \quad (16)$$

$$E_0 = E_0^b + \int dr' \overline{\overline{G}} \bullet Q^E E \quad (17)$$

$$\nabla \times \nabla \times H_0^b - k_b^2 H_0^b = \nabla \times J_s$$

$$\nabla \times \nabla \times E_0^b - k_b^2 E_0^b = \nabla \times M_s$$

Eqs.(16), (17) are not yet suitable solutions for  $H_0$  and  $E_0$ , since there is still a dependence on the unknown quantities  $H_*$  and  $E_*$ . We derive similar solutions for these fields, as

$$H_* = H_*^b + (\mu_b^*)^{-1} \nabla \times \int dr' \overline{\overline{G}} \bullet Q^E E \quad (18)$$

$$E_* = E_*^b + (\sigma_b^*)^{-1} \nabla \times \int dr' \overline{\overline{G}} \bullet Q^H H \quad (19)$$

$$H_*^b = (\nabla \times E_0^b - M_s) / \mu_b^*$$

$$E_*^b = (\nabla \times H_0^b - J_s) / \sigma_b^*$$

To proceed, we assume that the LN approach [1] is valid for the response (inductive modes are an extension). In this context, Eqs.(16),(17) are approximated by

$$H_0 \approx H_0^b + \overline{\overline{L}}^H H, \quad E_0 \approx E_0^b + \overline{\overline{L}}^E E \quad (20)$$

for the internal fields with

$$\overline{\overline{L}}^H = \int d'r \overline{\overline{G}} Q^H, \quad \overline{\overline{L}}^E = \int d'r \overline{\overline{G}} Q^E$$

Similarly, Eqs.(18) and (19) can be written as

$$E_* \approx E_*^b + \overline{\overline{P}}^H H, \quad H_* \approx H_*^b + \overline{\overline{P}}^E E \quad (21)$$

where we have introduced the new tensors

$$\overline{\overline{P}}^H = (\sigma_b^*)^{-1} \nabla \times \int dr' \overline{\overline{G}} Q^H, \quad \overline{\overline{P}}^E = (\mu_b^*)^{-1} \nabla \times \int dr' \overline{\overline{G}} Q^E$$

The physical field approximations are then obtained by summing Eqs.(20) and (21), yielding

$$E \approx E_b + \overline{\overline{L}}^E E + \overline{\overline{P}}^H H \quad (22)$$

$$H \approx H_b + \overline{\overline{L}}^H H + \overline{\overline{P}}^E E \quad (23)$$

$$E_b = E_0^b + E_*^b, \quad H_b = H_0^b + H_*^b$$

In terms of the LN scattering tensors

$$\overline{\overline{\Gamma}}^H = [ \overline{\overline{I}} - \overline{\overline{L}}^H ]^{-1}, \quad \overline{\overline{\Gamma}}^E = [ \overline{\overline{I}} - \overline{\overline{L}}^E ]^{-1}$$

we can rewrite Eqs.(22) and (23) as

$$E = \overline{\overline{\Gamma}}^E \overline{\overline{P}}^H H + \overline{\overline{\Gamma}}^E E_b \quad (24)$$

$$H = \overline{\overline{\Gamma}}^H \overline{\overline{P}}^E E + \overline{\overline{\Gamma}}^H H_b \quad (25)$$

Substituting (24) into (25), we obtain

$$H = \overline{\overline{M}}^H \left[ \overline{\overline{\Gamma}}^H H_b + \overline{\overline{\Gamma}}^H \overline{\overline{P}}^E \overline{\overline{\Gamma}}^E E_b \right] \quad (26)$$

$$\overline{\overline{M}}^H = \left[ \overline{\overline{I}} - \overline{\overline{\Gamma}}^H \overline{\overline{P}}^E \overline{\overline{\Gamma}}^E \overline{\overline{P}}^H \right]^{-1}$$

Note that in the DC magnetic case, there is no background electric field and the solution reduces to the static magnetic case suitable for simulating the response due to the earth's field.

## Extensions to Polyhedra

The LN theory (and its extensions to inductive modes, multi-body problems and permeability effects) is independent of scatterer or primitive geometry. It is only in the implementation where the geometry of the scatterer plays a significant role, particularly, in the evaluation of the scattering tensors ( $\overline{\overline{T}}_{ij}$  operators which include the  $\overline{\overline{\Gamma}}$  tensor). This is mathematically non-trivial for even the simplest primitive geometries. Our present developments allow the specification of a (generally non-convex) polyhedral anomaly. This is solved through a specialized triangle based polygon primitive which allows for a stable and rapid solution of even extremely complicated polygonal shapes.

## Examples:

### Resistivity and Induced Polarization:

As a first example, to show some basic but non-trivial capabilities, we draw upon a modeling exercise from municipal water pumping considerations. This example was specific to Southern Ontario but is easily adaptable to a more general aquifer geometry.

Over this area, there exists an aquifer at about 100m with a thickness of a few tens of meters underlain by a more resistive basement. This aquifer is used extensively for municipal water supplies for small towns and modest sized cities. Although the thickness of the aquifer is generally known, the aquifer contains non-permeable clay lenses. The distribution and quantity of these lenses could affect significantly the predicted safe pumping rate for the aquifer.

Figure 1 indicates the model. The survey is a 50m dipole-dipole array carried out at 7 frequencies between 0.1 and 100 Hz and over 4 survey lines (green) separated by 100m. There are four separate geometries for the lenses in the model. All 4 lenses have the same conductivity (1 S/m). All targets have the same chargeability and decay constant except the longest target which is non-polarizable. The red and purple targets are flat at 140m while the red target is at 105m. The blue target is dipping so that its bottom is at 140m. The original galvanic LN approximation extended to IP is utilizing for this modeling example.

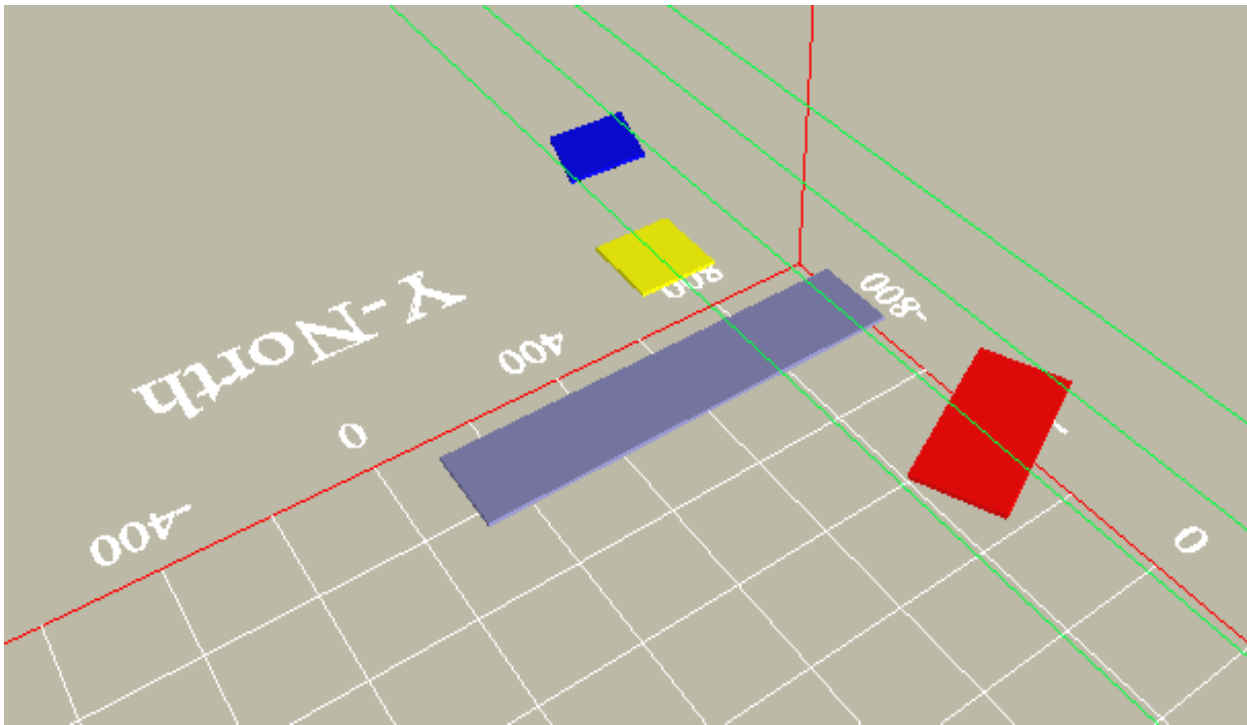


**Figure 1: Aquifer model**

The question we asked is whether the resistivity, alone, can distinguish the objects and if the targets' characteristics are distinguishable.

The model is easy to define and defining a reasonable sample grid is trivial. As can be seen from Figure 2, which shows the Resistivity for the  $N=6$  separation, the resistivity response does show all 4 targets, but the variations are too small to distinguish any structure in a realistic survey. At a separation of 300m, there is sufficient response variation but the objects are blurred together. The IP response (shown as phase angle) is more distinguishing (Fig. 3). However, the model exercise indicates that the short dipole separations and low frequencies give the primary differentiation. However, not until  $N=4$  and at relatively high frequencies ( i.e. 100Hz) is there sufficient phase variation to be realistically measurable in the noise. However, for these settings, the objects are again less distinguishable in the synthetic data.

The Induced Polarization-Resistivity model takes less than 5minutes on a standard Pentium II or III. It is, in summary, very simple and quick to define fully 3D Resistivity-IP targets and study response variation due to size, electric parameters and orientation.

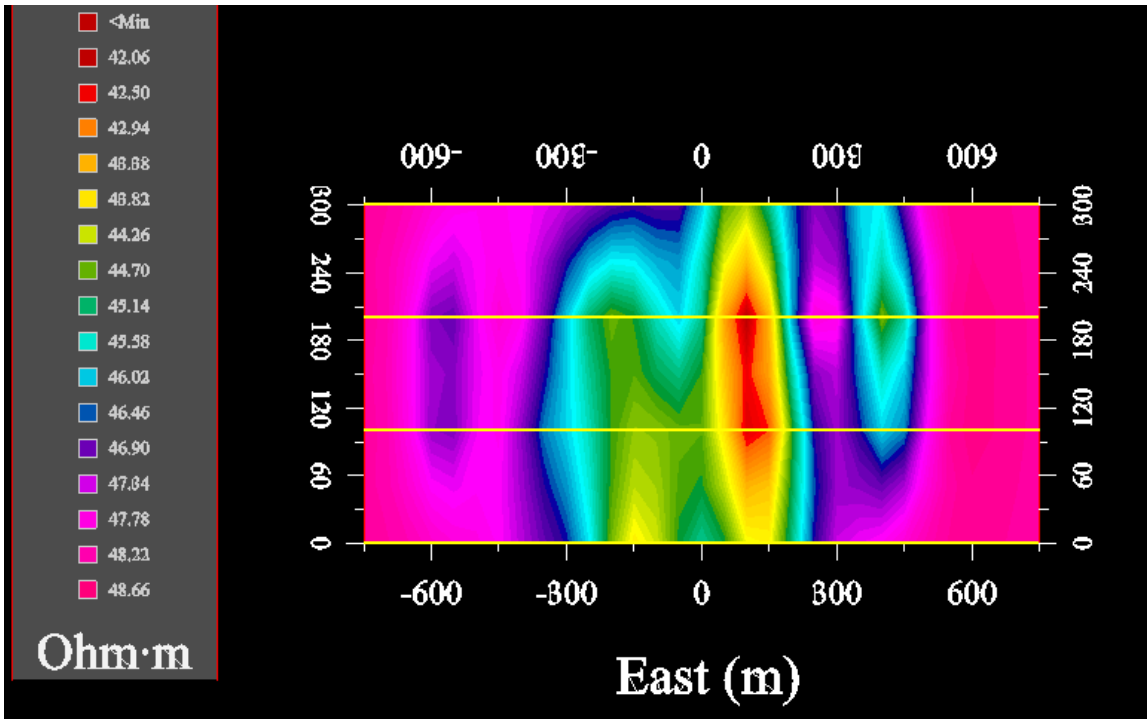


Figure 2: Resistivity Response, N=6

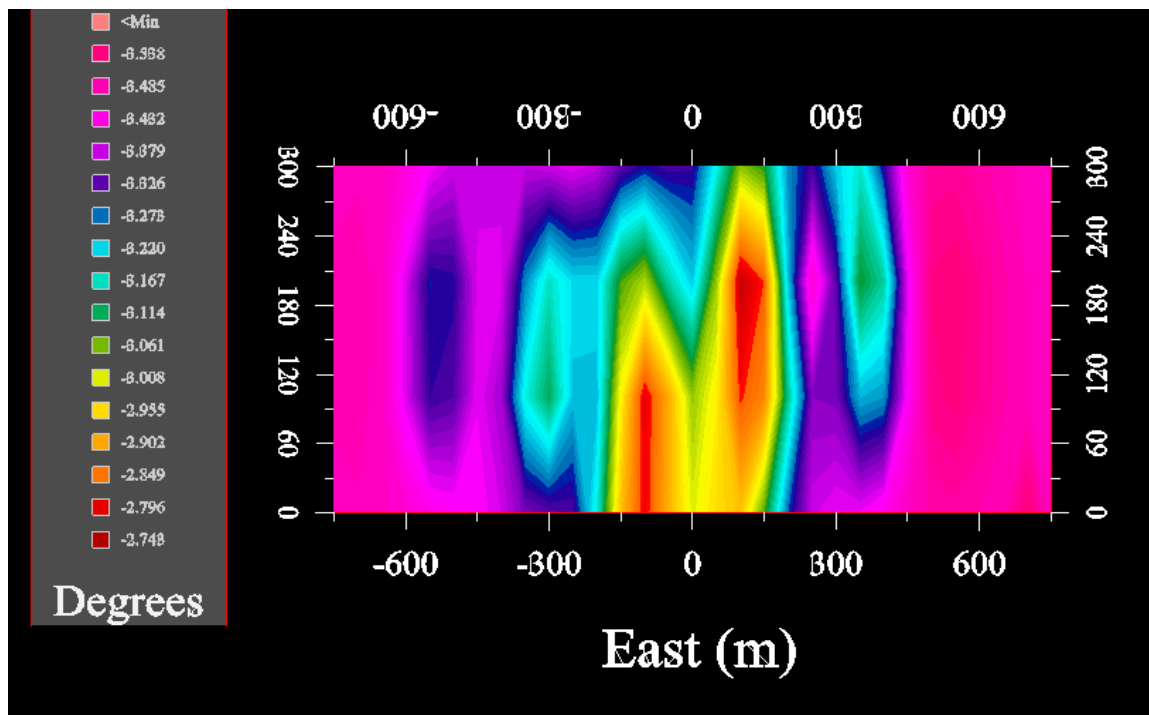


Figure 3: Induced Polarization Response : N=4, f=100Hz

### Clay Wedge – FEM Example:

For this exercise, we consider the response variations due to a clay wedge. For this example, we utilize both the polyhedra extensions and the extensions to higher order inductive terms (ILN). The model of the wedge is shown in Figure 4 (orange-red) with a rectangle (blue) for comparison. The host is represented as a thin resistive layer underlain by a 400 Ohm-m basement. The wedge is buried at 5m and is 100m by 50m thinning from 15m in thickness to the East. The wedge is given a Resistivity of 50 Ohm-m. The block has the same characteristics except that it has a constant thickness of 15m.

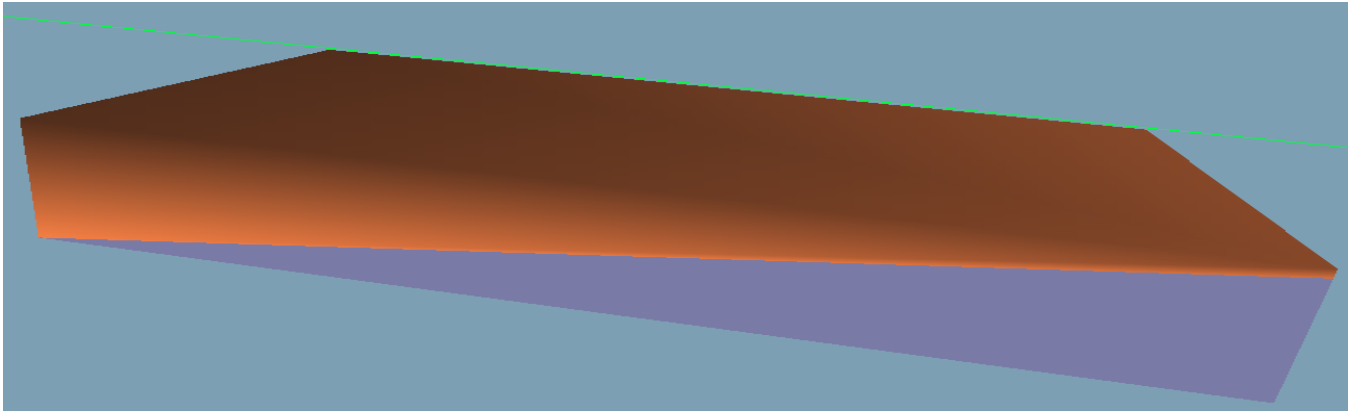


Figure 4: Clay Wedge Model

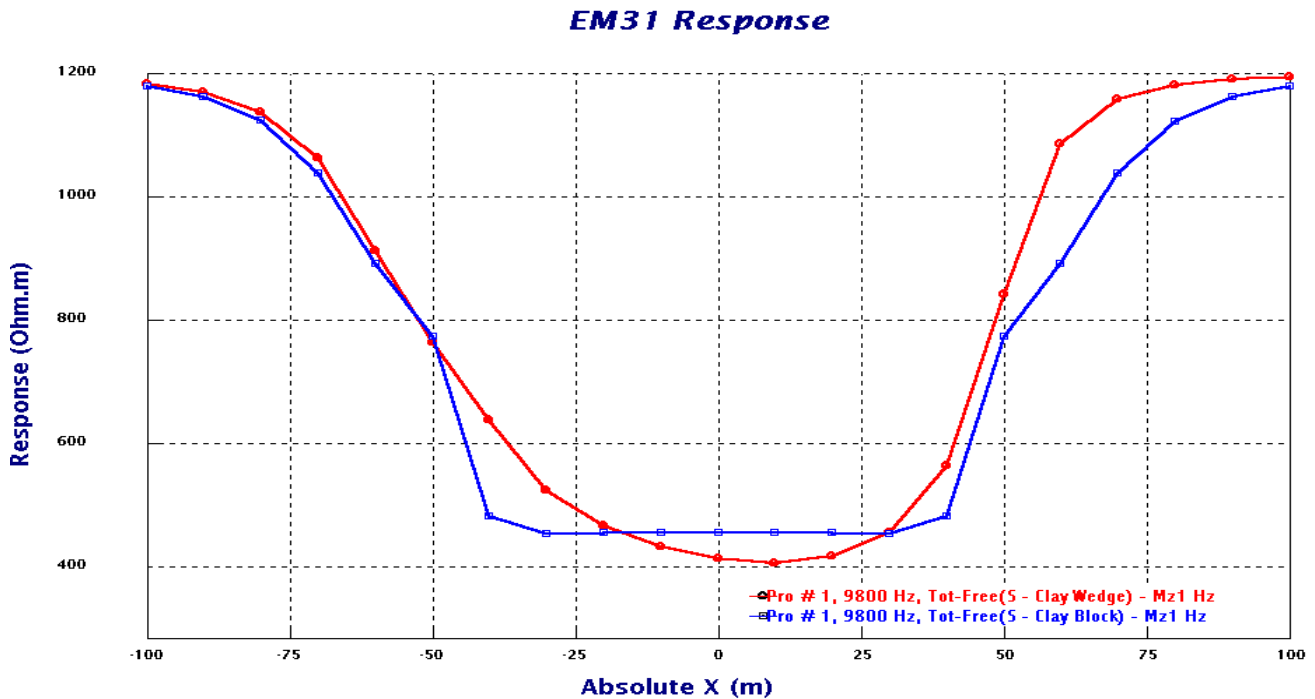


Figure 5: Clay Wedge vs Block EM31 Response

We examine the response to an EM31 system and show the comparison in Figure 5 where the wedge response is shown in Red and block in blue. We see an expected reduction in response as we move west but it is interesting that the short EM31 separation (3.66m) and the relatively high frequency ( 9800 Hz) shows significant differences in the response. All this indicates the necessity even with simple examples of the need to represent the true target geometry and proper simulation of inductive responses. Again, the simulation time is extremely rapid requiring only about 10 seconds on a 0.8GHz PIII computer.

## Conclusions

We have summarized various developments in rapid EM and magnetics modeling. As well, we have given only two examples of how this simulation capability can be utilized for near-surface applications. The simulations require only very standard computers and compute models accurately and rapidly in very short times. We believe that in the future these techniques will have increasing use in the environmental and geotechnical fields.

## References

- [1] T. M. Habashy, R. W. Groom and B. R. Spies, *Beyond the Born and Rytov Approximations: A Nonlinear Approach to Electromagnetic Scattering*, JGR, 98, no. B2 (1993).
- [2] I. R. Murray, *On Extending the Localized Non-Linear Approximator to Inductive Modes*, Extended Abstracts, F004, 59<sup>th</sup> EAGE Conference, Geneva, Switzerland (1997).
- [3] R. W. Groom and P. W. Walker and A.V. Dyck, *A Rapid Approximation to Three Dimensional Electromagnetic Scattering*, AEM Workshop, University of Arizona, Tucson (1993).
- [4] I. R. Murray\*, C. Alvarez and R. W. Groom, - *Modelling of complex electromagnetic targets using advanced non-linear approximator techniques*, Expanded Abstract, SEG, 1999